Adaptive Torque Ripple Control of Permanent Magnet Brushless DC Motors

Yilmaz Sozer David A. Torrey

Department of Electric Power Engineering
Rensselaer Polytechnic Institute Troy, NY 12180-3590
Voice: (518) 276-8297 Fax: (518) 276-6226

Abstract

This paper presents an approach for reducing the torque ripple of permanent magnet brushless dc motors. The technique requires coordination of an outer speed loop with an inner current loop. The inner current loop is responsible for shaping the phase currents during the commutation intervals. The outer speed loop is responsible for commanding the magnitude of the phase currents. It is shown that the speed loop must be sufficiently fast that the commanded phase current is able to respond to potential ripple torque during phase commutation; a simple direct adaptive controller satisfies this requirement. The inner current loop must be able to adaptively change the slope of the commanded current in order to avoid poor current regulation through inverter saturation in the face of large back emfs. The composite control is able to reduce torque ripple to a level which is dictated by phase ripple currents.

1 Introduction

Permanent magnet motors are becoming popular with continued cost reductions and performance improvements in permanent magnet materials. The main advantages of the permanent magnet motors are the high efficiency, high power density and the low maintenance cost due to the removal of the brushes [1], [2]. This paper is concerned with obtaining smooth torque output from a permanent magnet motor with full-pitch windings which create a trapezoidal back emf waveshape, a so-called permanent magnet brushless dc motor (PMBDC). The motor under consideration is typical of PMBDC motors in that the magnets are mounted on the surface of the rotor; each magnet pole is 180 electrical degrees in arc length.

Smooth torque output is essential for high performance speed and position control drives. The main sources for torque fluctuations in permanent magnet motors are cogging and ripple torque [3]. Cogging torque is created by the interaction of the permanent magnets with the stator teeth. The stator teeth create an angular variation in the reluctance of the magnetic circuit seen by the rotor magnets, thereby resulting in a reluctance torque. Ripple torque can be produced by reluctance torque or mutual coupling among phases and/or the rotor magnets. Reluctance torque is created in an interior permanent magnet motor due to the unequal direct and quadrature inductances of the rotor; the motor under consideration is not subject to reluctance torque, except that attributed to cogging.

Torque variations can result from the interaction of the magnet and the stator magnetomotive forces (mmf). Mutual ripple torques are created by the non-ideal behavior of the back emf voltages and the inability of the inverter to produce ideal currents, especially during phase commutations. This pulsating torque results in speed variations.

Previous efforts to produce smooth torque profiles can be put into two categories. The first category is focused on the design of the motor. The skewing technique falls into this category and has been shown to be very effective in suppressing cogging torque. The motor considered in this paper is built with a stator stack which is skewed one tooth pitch, effectively eliminating cogging torque.

The second category is focused on the control of the phase currents to suppress torque pulsations from cogging and ripple torques. Direct torque ripple control algorithms [4], production of the reference currents based on Fourier analysis [5], switching algorithms for commutation of the phase currents [6], [7] are applied to reduce pulsating torque production. These approaches have met with varying degrees of success.

This paper focuses on developing an active control algorithm to correct the pulsating torque production for the PMBDC motor. The algorithm supports synthesis of high bandwidth reference currents for each phase, coupled with techniques for ameliorating the effects of inverter saturation at high speeds. The high bandwidth

0-7803-4340-9/98/$10.00 © 1998 IEEE.

reference currents are created by a precise speed control algorithm based on a direct model reference adaptive controller (DMRAC) [8]. This algorithm provides precise, fast control in the face of varying motor and load parameters.

The inverter saturation problem is caused by the balanced nature of the motor phases and the difference in rising and falling times of the phase currents during commutation intervals in the face of the large back emfs encountered at higher speeds. This problem is solved by forcing the reference currents to have equal rising and falling slopes which are adjusted adaptively and automatically based on operating point with the minimum torque ripple and maximum efficiency. The block diagram of the PMBDC motor system is shown in Fig. 1.

Section 2 presents the generic model used to support control development for the PMBDC motor. Finite element analysis results are shown to provide the back emf profile of the PMBDC motor. The DMRAC algorithm and its application to the PMBDC motor is described in Section 3. Section 4 provides the algorithm for producing reference currents. Results are presented in Section 5. Conclusions and recommendations are in Section 6.

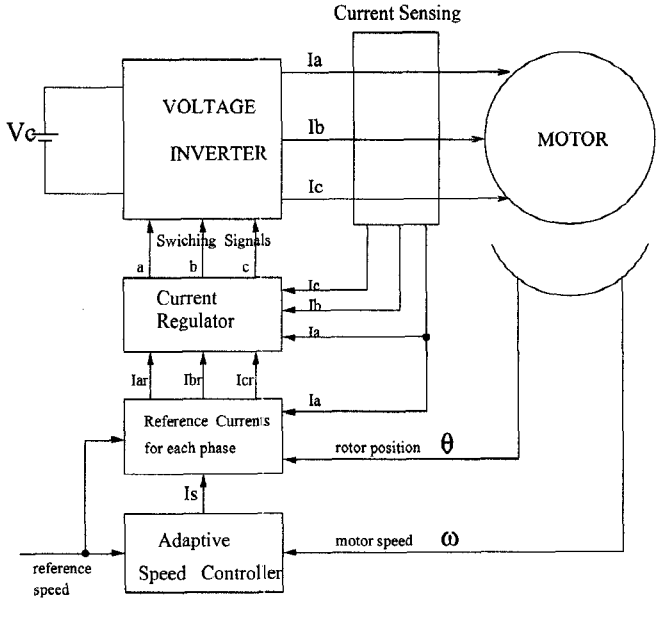

Figure 1: A block diagram for the direct model reference adaptive controller.

2 Modelling of PMBDC motor

A model which describes the dynamic behavior of the permanent magnet motor is needed to support control development. A lumped-parameter model of the PM motor is developed starting from basic electrical and mechanical equations.

The PMBDC motor consists of a stationary 3-phase stator winding and permanent magnets on the rotor. The stator windings of the PMBDC motor are wound such that the back emf of each phase is trapezoidal, implying mutual inductances between the stator and rotor are non-sinusoidal.

The circuit equations of the three windings in phase variables [1], [9] are

$$\begin{bmatrix} v_a \\ v_b \\ v_c \end{bmatrix} = \begin{bmatrix} R & 0 & 0 \\ 0 & R & 0 \\ 0 & 0 & R \end{bmatrix} \begin{bmatrix} i_a \\ i_b \\ i_c \end{bmatrix} + \frac{d}{dt} \begin{bmatrix} L_a & L_{ba} & L_{ca} \\ L_{ba} & L_b & L_{cb} \\ L_{ca} & L_{cb} & L_c \end{bmatrix} \begin{bmatrix} i_a \\ i_b \\ i_c \end{bmatrix} + \begin{bmatrix} e_a \\ e_b \\ e_c \end{bmatrix} \quad . \tag{1}$$

Assuming there is no change in rotor reluctances with angle, $L_a = L_b = L_c = L$ and $L_{ab} = L_{ca} = L_{cb} = M$. Since $i_a+i_b+i_c = 0$, and $Mi_b+Mi_c = -Mi_a$ the electrical dynamics for each phase are

$$\frac{di_x}{dt} = \left(\frac{1}{L-M}\right)[v_x - Ri_x - e_x] \quad , \tag{2}$$

where x denotes the phase a, b, or c. The mechanical dynamics are

$$J\frac{d\omega}{dt} = T_e - T_l - B\omega \tag{3}$$

$$\frac{d\theta}{dt} = \omega \quad , \tag{4}$$

where T_l is the load torque, B is the viscous damping and T_e is the electromagnetic torque which can be expressed as

$$T_e = \frac{e_a i_a + e_b i_b + e_c i_c}{\omega} \quad . \tag{5}$$

The ideal phase current waveform is rectangular in which the current pulses are 120 electrical degrees wide and of magnitude I_s. With 180 degree (electrical) magnet arcs, the width of the flat top of the back emf waveform is greater than 120 degrees with the magnitude of E_s as shown in Fig. 2. Assuming there is no phase difference between current and back emf we can write the electromagnetic torque as

$$T_e = \frac{2E_s I_s}{\omega} \quad . \tag{6}$$

The control technique is studied through application to a 30 hp surface magnet non-salient PMBDC motor. Finite element analysis of this motor shows that the assumed model for the PMBDC motor is valid in terms of phase and the mutual inductances but the flat top portion

of the back emf wave shape is less than 120 electrical degrees. Figure 3 shows the three phase back emf voltages for the 30 hp PMBDC motor.

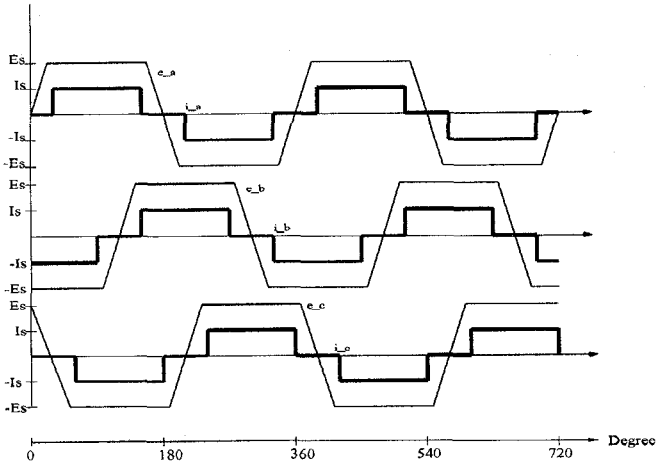

Figure 2: The ideal three phase stator currents and back emfs.

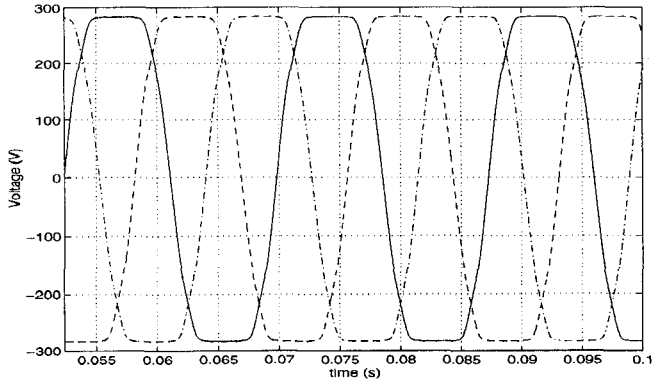

Figure 3: Three phase back emf voltages, based on finite element analysis of the PMBDC.

3 DMRAC Algorithm

The linear time invariant model reference adaptive control problem is considered for the plant

$$\begin{aligned} \dot{x}_p(t) &= A_p x_p(t) + B_p u_p(t) \\ y_p(t) &= C_p x_p(t) \quad , \end{aligned} \tag{7}$$

where $x_p(t)$ is the $(n \times 1)$ state vector, $u_p(t)$ is the $(m \times 1)$ control vector, $y_p(t)$ is the $(q \times 1)$ plant output vector, and A_p, B_p are matrices with appropriate dimensions based upon possibly varying parameters.

The objective is to find, without explicit knowledge of A_p and B_p, the control $u_p(t)$ such that the plant output vector $y_p(t)$ follows the reference model

$$\begin{aligned} \dot{x}_m(t) &= A_m x_m(t) + B_m u_m(t) \\ y_m(t) &= C_m x_m(t) \quad . \end{aligned} \tag{8}$$

The model incorporates the desired behavior of the plant, but its choice is not restricted. In particular, the order of the plant may be much larger than the order of the reference model.

The adaptive control law based on the command generator tracker (CGT) approach [10] is given as

$$u_p(t) = K_e(t) e_y(t) + K_x(t) x_m(t) + K_u(t) u_m(t) \quad , \tag{9}$$

where $e_y(t) = y_m(t) - y_p(t)$ and $K_e(t)$, $K_x(t)$, and $K_u(t)$ are adaptive gains. Defining the vector $r(t)$ as

$$r(t) = [e_y(t)\, x_m(t)\, u_m(t)]^T \quad , \tag{10}$$

the control $u_p(t)$ is written in a compact form as $u_p(t) = K(t) r(t)$ with

$$\begin{aligned} K(t) &= K_p(t) + K_i(t) \\ K_p(t) &= e_y(t) r^T(t) T_p, \quad T_p \geq 0 \\ \dot{K}_i(t) &= e_y(t) r^T(t) T_i, \quad T_i > 0 \quad ; \end{aligned} \tag{11}$$

T_p and T_i are arrays of proportional and integral weights, respectively. The block diagram of the DMRAC is shown in Fig. 4.

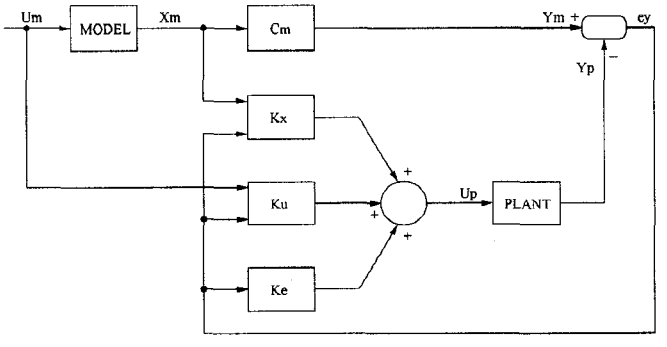

Figure 4: A block diagram for the direct model reference adaptive controller.

The gains in the DMRAC controller adapt themselves to reduce the error between model and the plant output. Adaptation stops when the error goes to zero. The plant state x_p and plant output y_p are each equal to the speed ω, and the adaptive control u_p is the current magnitude I_s. Three phase reference currents are produced based on the rotor position θ and the magnitude of the control I_s.

A first order model is chosen to provide fast control response. The difficulty is in adjusting the six integral and proportional weights T_p and T_i to get a smooth torque

profile. Small weights give error in model tracking and increased torque ripple. Large weights increase sensitivity to inverter switching. The integral and the proportional weights are adjusted to get smooth torque output with acceptable operation.

4 Algorithm for Current References

As shown in Fig. 2 mutual torque ripple is zero for ideal quasi-square three phase currents and trapezoidal back emf voltages having the flat top portion greater than 120 electrical degrees. The finite element analysis results show that the flat top portion of the back emf voltage is less than 120 electrical degrees (Fig. 3). Since the voltage across the motor phase windings is limited by the inverter and the back emf voltages, there is a certain rise and fall time for the phase currents. The rising and falling times of the currents are not equal since the available voltages across each winding are different.

At low speeds the rising phase current i_1 reaches the required level before the falling phase current i_2 reaches zero. The magnitude of the voltage across the falling phase is much greater than that for the rising phase at high speeds, so the phase current i_1 drops to zero before the phase current i_2 reaches to required level [11]. The motor phases are Y connected and the three phase currents sum to zero at all times. This makes the inverter saturate during the switching of the phase currents. The commanded currents cannot be produced with the saturated inverter. Fluctuations occur in the current and torque profile. The output motor speed is also affected by these fluctuations [12]. Examples of the commutation currents and torque spikes are shown in Figs. 5 and 6.

Since controlling the phase currents with one current sensor is effective in reducing cost, some authors applied their solutions to reduce the torque ripple with two phase systems [6]. Later an extra current sensor is used to prevent the loss of current regulation. It prevents the torque ripple at low speed, but it is still there for high speeds. A recent study [7] describes the new method to reduce high speed torque ripple with a new regulation technique. Since the nature of the controller requires keeping the third phase current constant during the commutation of the other phases, the torque profile deteriorates when the flat top of the back emf is smaller than 120 electrical degrees.

We approach the problem by designing the reference currents to be of a shape which can be supported by the inverter so that the outer speed loop and the inner current loop work harmoniously. We force the commanded currents to have the same rising and falling slopes. As shown in Fig. 7, the rising and falling phases start commutating β degrees before the ideal commutation angle. The commutation interval is carried out over an angle of 2β so the slope of the reference currents are $\frac{I_s}{2\beta}$. I_s is the output of the adaptive controller which is required to get desired speed output with the minimum torque ripple. The slope rate is set by the motor operating conditions. Table 1 provides an analytic expression of the reference currents for each regions identified in Fig. 7.

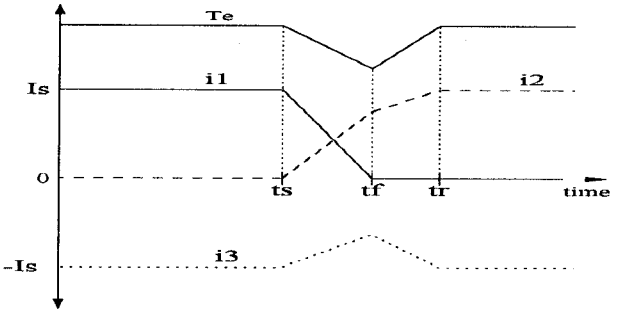

Figure 5: Three phase commutation currents at high operating speeds.

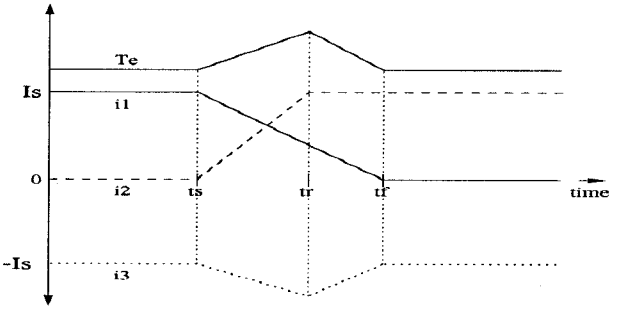

Figure 6: Three phase commutation currents at low operating speeds.

The slope angle β is set by the output of an integrator which holds the value of time over which the actual current is unable to follow the commanded current. After a couple cycles β reaches a value that allows the phase current to follow the command. Any increases in the reference speed or the load reflect themselves as an increase in the current command. Increasing the current command or the back emf voltages causes the phase currents to deviate from the commanded currents, thereby starting the integrator to further increase β. If the speed reference or load torque are decreased by a certain amount, the integrator is reset ($\beta = 0$) and, if necessary, β reaches its required value after integration for a couple of cycles. The block diagram of the automatic adjustment of the β is shown if Fig. 8. The goal is to operate with the minimum value of β at all times for increased drive efficiency.

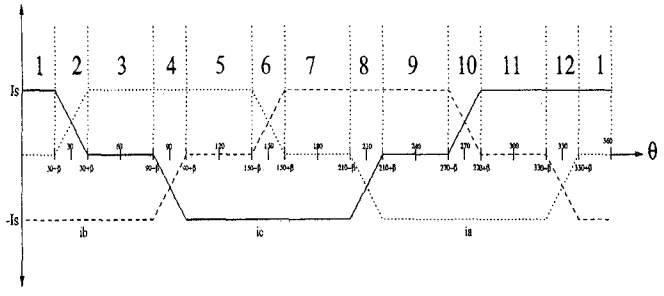

Figure 7: Three phase reference currents with rising and falling slopes.

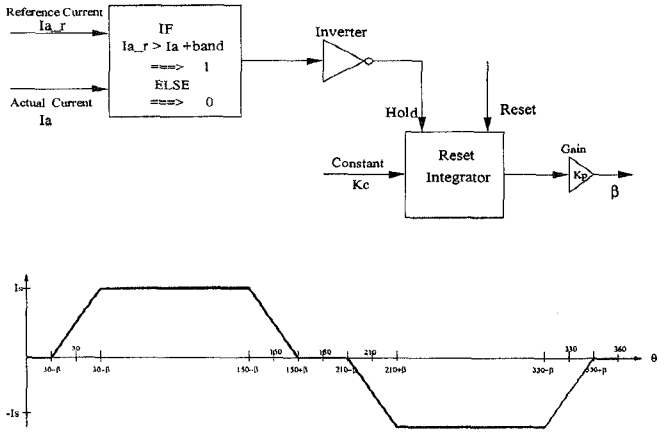

Figure 8: Automatic adjustment mechanism for angle β.

5 Simulation Results

The control development is tested through the careful simulation of a commercial 30 hp PMBDC motor with the parameters obtained from the finite element analysis as shown in Fig. 3. The switching actions of the three-phase voltage source inverter, DMRAC controller and motor model are simulated to carefully show the improvements obtainable in motor torque production. A hysteretic current regulator having a hysteresis band of 0.7 A is used to produce motor phase currents. The performance of the reference currents with the adaptive slope is compared with the quasi-square reference currents for 120 rad/s and 185 Nm load torque.

Figures 9 - 11 show the performance of the motor for 120 rad/s and 185 Nm load torque with the quasi-square reference current. As shown in Fig. 9 the inverter saturates during the switching of the phases, and the phase currents cannot follow the commanded currents. The controller responds by requiring additional current to reduce the speed error. Peak to peak torque ripple reaches up to 60 Nm as shown in Fig. 11.

Figures 12 - 16 show the performance of the motor for 120 rad/s and 185 Nm load torque with the quasi-square reference current having adaptive slope. β reaches 16.4° for this operating point as shown in Fig. 15. The torque ripple is reduced to around 4.63 Nm as shown in Fig. 16 which is around 2% of the rated torque. Since K_v is approximately 2.5 Vs/rad and the approximate value of T_e is $2K_v I_s$, the torque ripple due to the hysteretic band is around 3.5 Nm. This ripple can, of course, be further reduced by inserting a low pass filter between the inverter and the motor.

It is worth noting in Figs. 12 and 14 how the commanded phase current increases during the commutation interval. This increased current is compensating for the drop in torque production due to commutation between the other phases. This suggests how the adaptive speed controller works with the inner current controller in order to substantially eliminate torque variation. It also suggests that the adaptive controller must have sufficiently fast response.

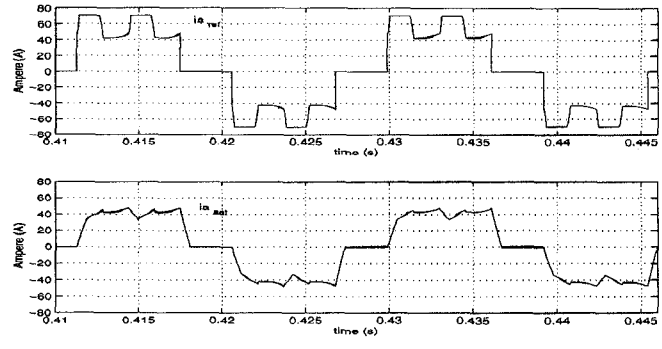

Figure 9: The reference current from adaptive controller shaped without slope adjustment and the motor current for phase a.

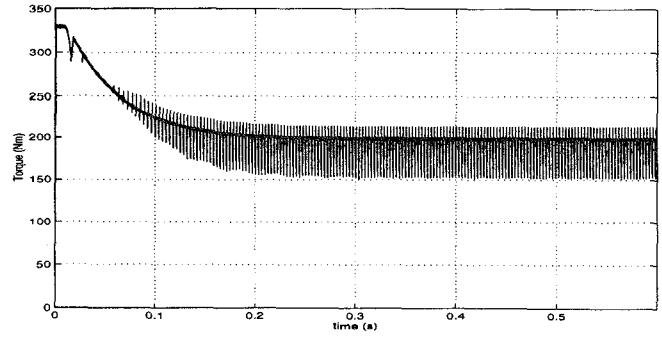

Figure 10: Transient torque profile of the PMBDC motor without slope adjustment on the reference.

Table 1: Analytic expressions for the reference currents for each region of Fig. 7, where $m = I_s/(2\beta)$.

Region	i_a	i_b	i_c
1	0	$-I_s$	I_s
2	$m(\theta-(30-\beta))$	$-I_s$	$I_s - m(\theta-(30-\beta))$
3	I_s	$-I_s$	0
4	I_s	$-I_s + m(\theta-(90-\beta))$	$-m(\theta-(90-\beta))$
5	I_s	0	$-I_s$
6	$I_s - m(\theta-(150-\beta))$	$m(\theta-(150-\beta))$	$-I_s$
7	0	I_s	$-I_s$
8	$-m(\theta-(210-\beta))$	I_s	$-I_s + m(\theta-(210-\beta))$
9	I_s	I_s	0
10	$-I_s$	$I_s - m(\theta-(270-\beta))$	$m(\theta-(270-\beta))$
11	$-I_s$	0	I_s
12	$-I_s + m(\theta-(330-\beta))$	$-m(\theta-(330-\beta))$	I_s

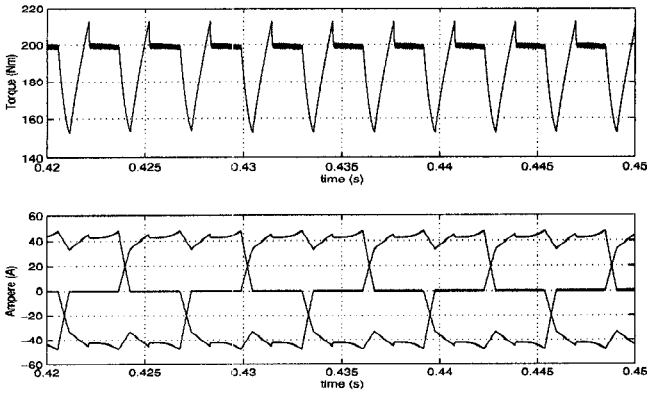

Figure 11: The profiles for the torque and the three phase motor currents without slope adjustment on the reference.

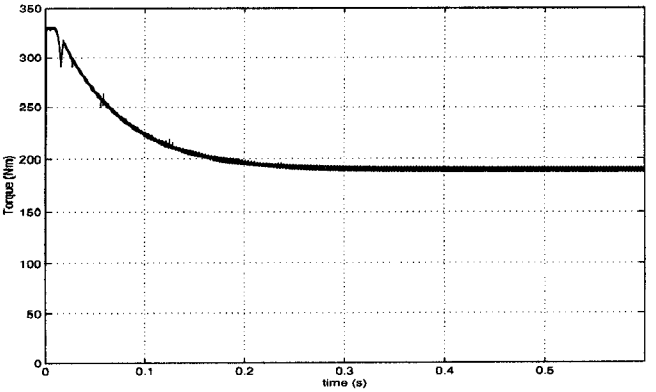

Figure 13: Transient torque profile of the PMBDC motor with slope adjustment on the reference.

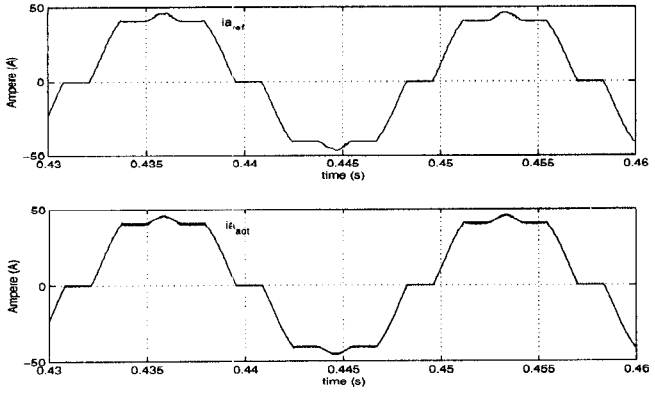

Figure 12: The reference current from adaptive controller shaped with slope adjustment and the motor current for phase a.

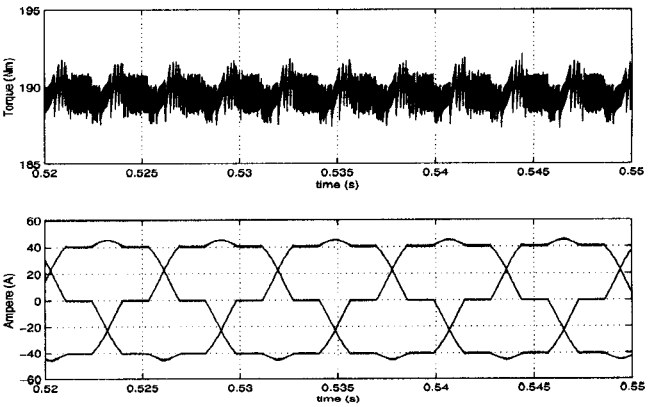

Figure 14: The profiles for the torque and the three phase motor currents with slope adjustment on the reference.

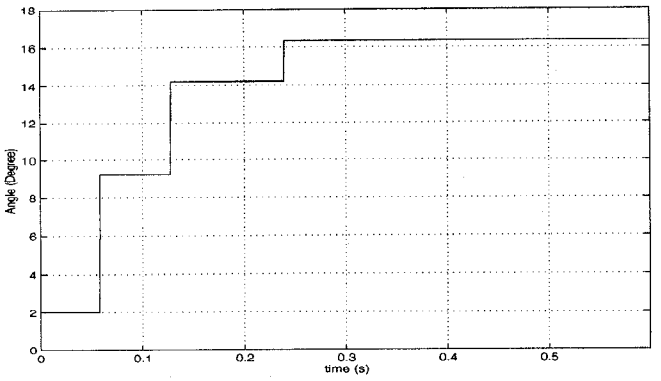

Figure 15: Adjustment of the angle β.

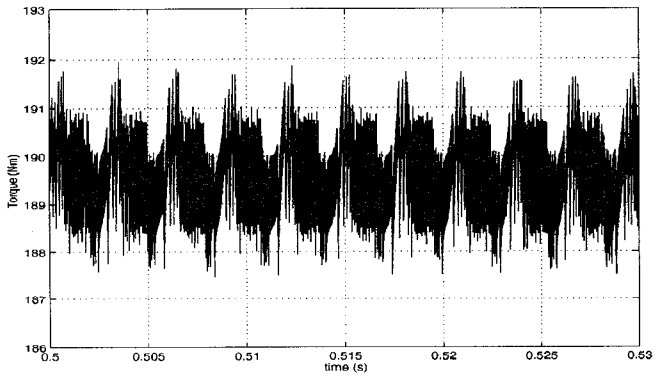

Figure 16: Steady state torque profile of the PMBDC motor with slope adjustment on the reference.

6 Summary

This paper has presented an approach for reducing the torque ripple of permanent magnet brushless dc motors. The technique requires coordination of an outer speed loop with an inner current loop. The inner current loop is responsible for shaping the phase currents during the commutation intervals. The outer speed loop is responsible for commanding the magnitude of the phase currents.

The speed loop must be sufficiently fast that the commanded phase current is able to respond to the potential decrease in torque output during commutation if the phase current command is held constant. This paper has shown that a simple direct adaptive controller is sufficiently fast to serve as the speed controller. The inner current loop must be able to adaptively change the slope of the commanded current in order to avoid poor current regulation through inverter saturation.

References

[1] T.J.E. Miller, *Brushless Permanent-Magnet and Reluctance Motor Drives*, Clarendon Press, Oxford 1989.

[2] D. C. Hanselman, *Brushless Permanent-Magnet Motor Design*, McGraw-Hill, Inc., 1994.

[3] T. M. Jahns and W. L. Soong, "Pulsating torque minimization techniques for permanent magnet AC motor drives-a review," *IEEE Trans. Ind. Elec.*, Vol.43 No. 2, pp. 321-330, April 1996.

[4] T. S. Low, T. H. Lee, K. J. Tseng, K. S. Lock, "Servo performance of a BLDC drive with instantaneous torque control," *IEEE Trans. on Ind. Appl.*, Vol.28, No.2, pp. 455-462 , March/April 1992.

[5] D. C. Hanselman, "Minimum torque ripple, maximum efficiency excitation of brushless permanent magnet motors" *IEEE Trans. Ind. Elec.*, Vol. 41, No. 3, pp. 292-300, June 1994.

[6] Y. Murai, Y. Kawase, K. Ohashi, K. Nagatake, K. Okuyama, "Torque ripple improvement for brushless DC miniature motors," *IEEE Trans. Ind. Appl.*, Vol.25, No.3, pp. 441-450, May/June 1989.

[7] J. Cros, J. M. Vinassa, S. Clenet, S. Astier, M. L. Mazenc, "A novel current control strategy to minimize torque ripples due to phases commutations" *Eur. Conf. Power Elect. Appl.*, Vol.4, pp. 266-271, Brighton, 1993.

[8] Y. Sozer, H. Kaufman, and D. A. Torrey, "Direct model reference adaptive control of permanent magnet brushless dc motors," *IEEE Int. Conf. on Control Appl.*, Vol. 1, pp. 633-638, Hartford, Oct. 1997.

[9] P. Pillay and R. Krishnan, "Modelling, simulation, and analysis of permanent-magnet motor drives," *IEEE Trans. Ind. Appl.*, Vol. 25, No.2, pp. 265-278, 1989.

[10] H. Kaufman, I. Bar-kana, and K. M. Sobel, *Direct Adaptive Control Algorithms: Theory and Applications*, Springer-Verlag, New York, 1994.

[11] R. Carlson, M. L. Mazenc, J. C. dos. S. Fagundes "Analysis of torque ripple due to phase commutation in brushless DC machines," *IEEE Ind. Appl. Soc. Annu. Meet.*, Vol.1, pp. 287-292, Seattle, Oct. 1990.

[12] T. M. Jahns, "Torque production in permanent-magnet synchronous motor drives with rectangular current excitation" *IEEE Trans. on Ind. Appl.*, Vol. IA-20, No. 4, pp. 803-813, 1984.